Supporting Information

Combined "Grass Grid" and "Reverse Biomineralization" Boosts the Powder Anode Utilization of Zn-Air Batteries

Haitao Zheng[a], Yu Bai[a], Yuchao Wang[a], Jing Zhang[a], Meng Wang[a], Yingbi Chen[a], Guozhao Fang[b], and Yongpeng Lei*[a]

[a]State Key Laboratory of Powder Metallurgy, Central South University, Changsha 410083, China; E-mail: lypkd@163.com; leiyongpeng@csu.edu.cn

[b]School of Materials Science and Engineering, Central South University, Changsha 410083, China

Materials and Methods

Chemicals and materials. Zn powder (800 mesh) was purchased from Hunan New Welllink Advanced Metallic Material Co., Ltd., Zn powder (100 mesh) was purchased from Gansu Yellow River Zn Products. E-44 Epoxy resin was purchased from Guangzhou Dongfeng Chemical Industrial Co., Ltd. Conductive carbon black (Super C45), Carbon nanotube (CNT-3213) and Conductive graphite (KS-6) was purchased from Guangdong Candlelight New Energy Technology Co., Ltd, Dodecyl dimethyl betaine (BS-12 30 wt% in water) Polytetrafluoroethylene emulsion (PTFE, 60%), Polyvinylidene fluoride (PVDF), Carboxymethyl cellulose (CMC), Polyethylene glycol 400 (PEG) were purchased from Macklin. A Zn plate (thickness of 0.3mm) was purchased from Shanghai Maikelong Co., Ltd. Milli-Q water (18.2 MΩ) was obtained from the Milli-Q system (UPT). Waterproof breathable membrane and Ni foam were purchased from Changsha Spring New Energy Technology Co., Ltd. Potassium hydroxide (KOH, AR), Anhydrous ethanol were purchased from Sinopharm Chemical Reagent Co., Ltd, China. All chemicals were from commercial sources and used without further purification. Zhi Li Yinyue A13 ZABs were purchased from Zhuhai Zhi Li Battery Co., Ltd. Extra Power ZABs were purchased from WS Audiology Switzerland AG. Pt/C catalyst was purchased from Johnson Matthey Japan G.K.

Synthesis of Zn powder anode (Z_p). First, 0.5 g E-44 was dissolved in 5 mL of anhydrous ethanol under magnetic stirring. Then, 2.5 mg Zn powder (800 mesh) and 50 mg of Super C45 were added to the E-44 solution, stirring for another 30 min to precipitate. Subsequently, the obtained Zn powder slurry was spin-coated onto nickel foam with a porous conductive substrate of 70 mm(length)×30 mm(width)×3 mm(thickness), and the solvent was dried in a drying oven at 60℃ to obtain the anode layer, noted as Z_p. The preparation methods of the powder anodes for the two types of waste materials are the same, except that 1 g of the waste material is used. The Z_p electrode was immersed in the BS-12 aqueous solution for 1 hour, which was denoted as Z_p+BS-12.

Fabrication of an air cathode. 60 mg of the Pt/C catalyst was mixed and ground thoroughly with 10 mg of carbon powder in a small amount of ethanol. Subsequently, 100 μL of PTFE solution was added, and the mixture was further ground to homogeneity. The resulting slurry was fabricated into electrode sheets with a thickness of 0.2 mm and a dimension of 1.0×1.0 cm^2. Afterwards, the electrode sheet, a waterproof and breathable membrane, and nickel foam were compressed together. The catalyst loading was controlled at 2 mg cm^{-2}.

Assembly and measurement of Liquid ZABs. After the positive and negative electrodes were prepared and assembled, respectively, 70 mL of 6 mol L^{-1} KOH and 10 μL of BS-12 electrolyte were poured into a Zn powder air battery (denoted as GG+RB). GG, GG+RB-9, and GG+RB-10 were synthesized via the same procedure as that of GG+RB, except 0, 5, and 25 μL of BS-12 were added, respectively. 100 mesh Zn powder used to replace 800 mesh was named GG+RB-1. GG+RB-2, GG+RB-3, and GG+RB-4 were synthesized via the same procedure as that of GG+RB, except 0.2 g, 1.0 g, and 1.5 g of E-44 were added, respectively. GG+RB-5 and GG+RB-6 were synthesized via the same procedure as that of GG+RB, except 0 mg and 100 mg of carbon black were added, respectively. GG+RB-7 and GG+RB-8 were synthesized via the same procedure as that of GG+RB, except 50 mg of Carbon nanotubes CNT-3212 and 50 mg conductive graphite KS-6 were added, respectively. Zn plates were assembled with ZABs in the same way, which were recorded as Zn plate/KOH and Zn plate/RB. In addition, ZABs with different binders (PEG, CMC, PTFE, PVDF) were compared and recorded as PEG/RB, CMC/RB, PTFE/RB, and PVDF/RB. The recipe list is given in Table 1.

Assembly and measurement of waste powder battery. The preparation method for the waste powder anode was consistent with that described earlier for Z_p, except that 1.5 g of waste material, 0.1 g of E-44, and 0.02 g of Super C45 were used. The prepared anode was then assembled following the same method as described above for liquid ZABs.

Material characterization. X-ray diffraction (XRD) profiles were performed on a D8 Advance X-ray diffractometer using Cu Kα radiation at 25℃. X-ray Photoelectron Spectroscopy (XPS) experiments were conducted on Thermo K-alpha X-ray photoelectron spectroscopy with Mono Al Kα radiation. FT-IR spectra of the solid state were evaluated by a Nicolet 5700 FT-IR. Contact angle measurements of the Zn electrode were performed by a contact angle measurement system (CA100D, Yinnuo). The morphologies of the Zn anodes were examined using SEM (Hitachi SU 70 microscope, operating voltage = 5 kV). 1H nuclear magnetic resonance (NMR) spectra were recorded on Bruker Avance Neo 400WB or Bruker 400MHz. The 3D CLSM topographic images were analyzed with a Bruker Nano Surfaces Division (CN12340896). The Zeta potentials were collected using Zetasizer NANO ZS90. Atomic force microscopy (AFM) and Kelvin probe force microscope (KPFM) experiments were carried out using Bruker multimode 8. Electron probe microanalysis was carried out on the EPMA-1720 instrument with wavelength-dispersive X-ray spectroscopy characterization. The bubble generation process was monitored on-site using an optical microscope (LEIKA DM2700 M). XRD pole figure measurements were conducted on a D8 Advance X-ray diffractometer equipped with a texture attachment, using Cu Kα radiation at room temperature. Elemental analysis (EA) for carbon, hydrogen, nitrogen, and sulfur (CHNS) was performed using an Elementar vario MICRO cube analyzer. Electron backscatter diffraction (EBSD) and inverse pole figure (IPF) mapping were carried out using a field-emission scanning electron microscope (FE-SEM, Model SU5000) equipped with an EBSD detector, operating at an acceleration voltage of 20 kV.

Electrochemical evaluation and battery measurement: Tafel curve, HER measurements, and OCP were carried out in a conventional three-electrode system on a CHI 660 electrochemical station (Shanghai Chenhua, China). The prepared Zn powder anode (Z_P) with a geometric area of 1 cm^2 was used as the working electrode, and a pure Zn plate (99.99%) with the same area was used as Comparison samples. The counter electrode and the reference electrode were a graphite rod electrode and a saturated calomel electrode (SCE), respectively. A

6 M KOH aqueous solution was used as the alkaline electrolyte. For the BS-12-containing electrolyte, 0.55 mM BS-12 was added to 6 M KOH and magnetically stirred for 30 min to form a homogeneous solution. The Tafel polarization curves potential scan range was set to -1.8 V to -1.2 V with a scan rate of 10 mV s^{-1}. Before testing, the working electrode was stabilized in the electrolyte for 10 min to eliminate the influence of electrode surface adsorption and reach an OCP steady state. The HER was measured in the range of -1.48 V to -2.5 V with a scan rate of 1 mV/s. The electrochemical impedance spectroscopy (EIS) tests were carried out at 0.050 V vs OCP. The spectra were recorded in a frequency range from 10^{-2} to 10^{6} Hz with a voltage amplitude of 5.0 mV.

The power density (P) was measured on the CHI 730E workstation for the Zn-air battery through LSV testing. The scan rate was 5 mV/s, and the potential range was from 0 V to 1.6 V. The calculation formula was:

$$P\ (mW\ cm^{-2}) = J\ (mA\ cm^{-2}) \times V\ (V)$$

where J is the discharge current density, and V is the corresponding discharge voltage. The peak power density was extracted from the power density-current density curve.

Constant current discharge using NEWARE testing equipment at 20/100/5 mA cm^{-2} until the battery voltage drops to 0.5 V (cut-off voltage), record the discharge curve, and calculate the specific capacity and Zn utilization rate. Both the current density (mA/cm^2) was normalized to the effective surface area of the air cathode. The specific capacity and the utilization rate of Zn were calculated according to the equation below:

$$\text{Specific capacity} = \frac{\text{current density} \times \text{service hours}}{\text{weight of consumed Zn}}$$

$$\text{The utilization rate of Zn} = \frac{\text{Actual specific capacity}}{\text{Theoretical specific capacity (820 mAh/g)}}$$

$$\text{Electric energy output} = \text{current} \times \text{service hours} \times \text{average voltage}$$

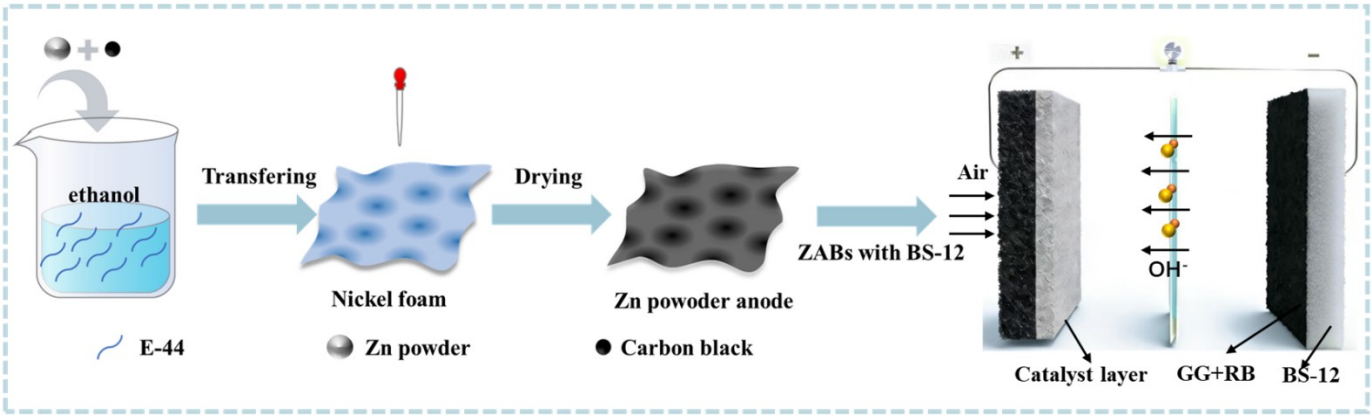

Figure S1. Schematic preparation procedure of Zp and GG+RB.

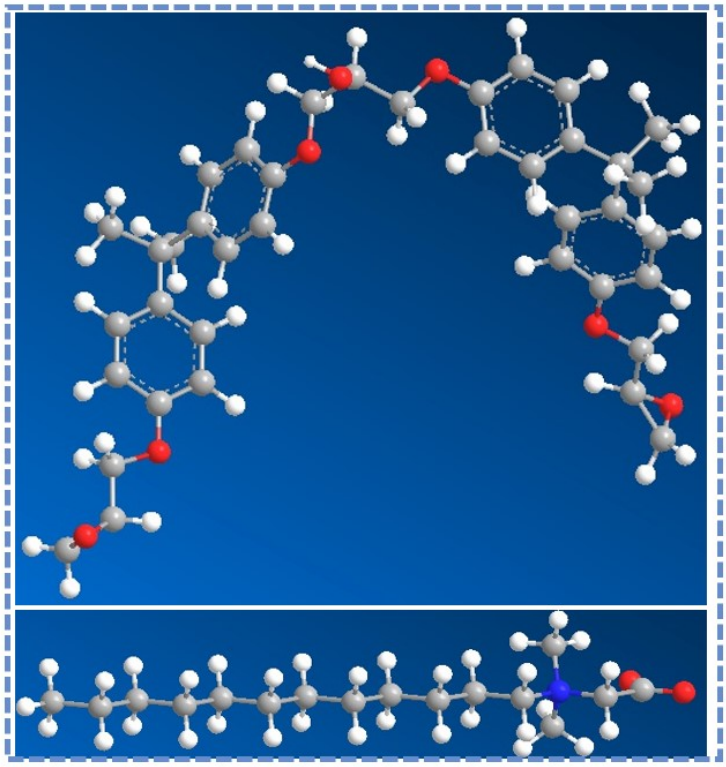

Figure S2. (a) E-44 and (b) BS-12 Molecular Formula Stick Model (The blue, red, gray, and white balls represent the N, O, C, and H elements, respectively.

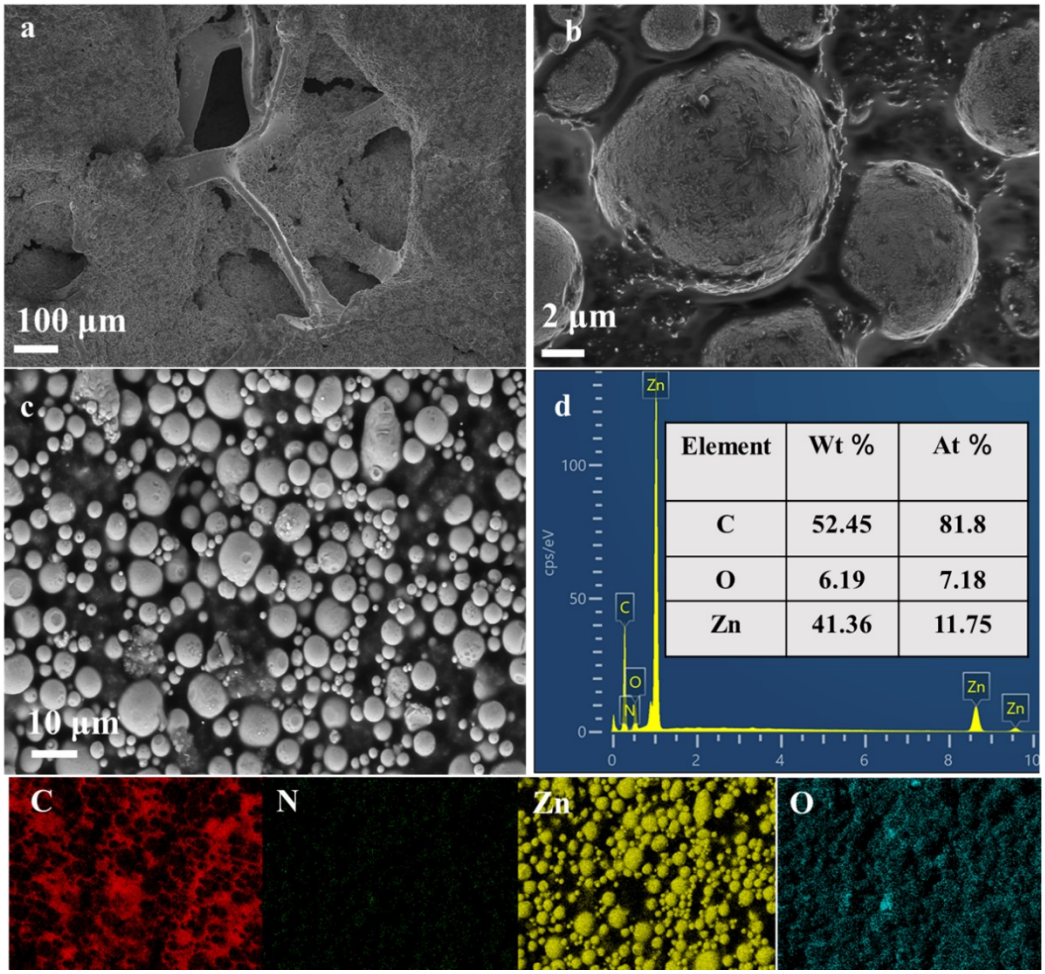

Figure S3. (a,b) SEM and (c,d) EDS mapping of Z_P.

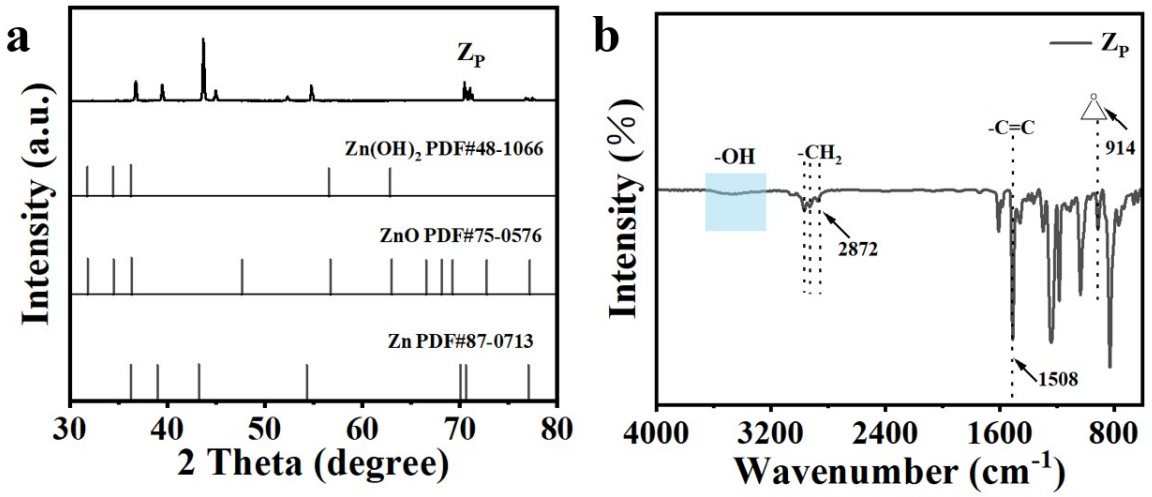

Figure S4. (a) XRD and (b) FTIR of Z_P.

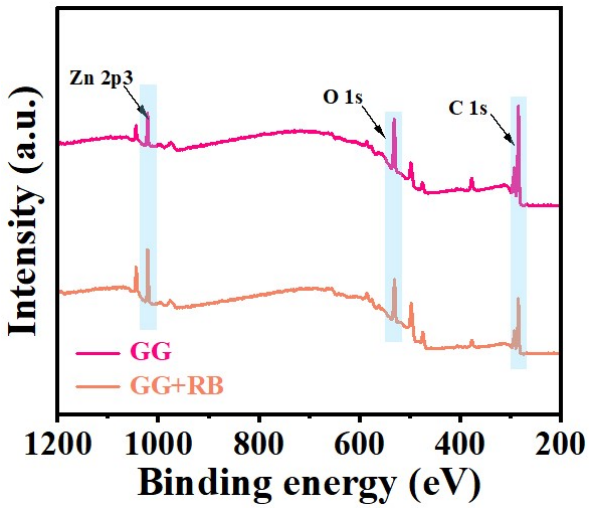

Figure S5. XPS spectrum of GG and GG+RB.

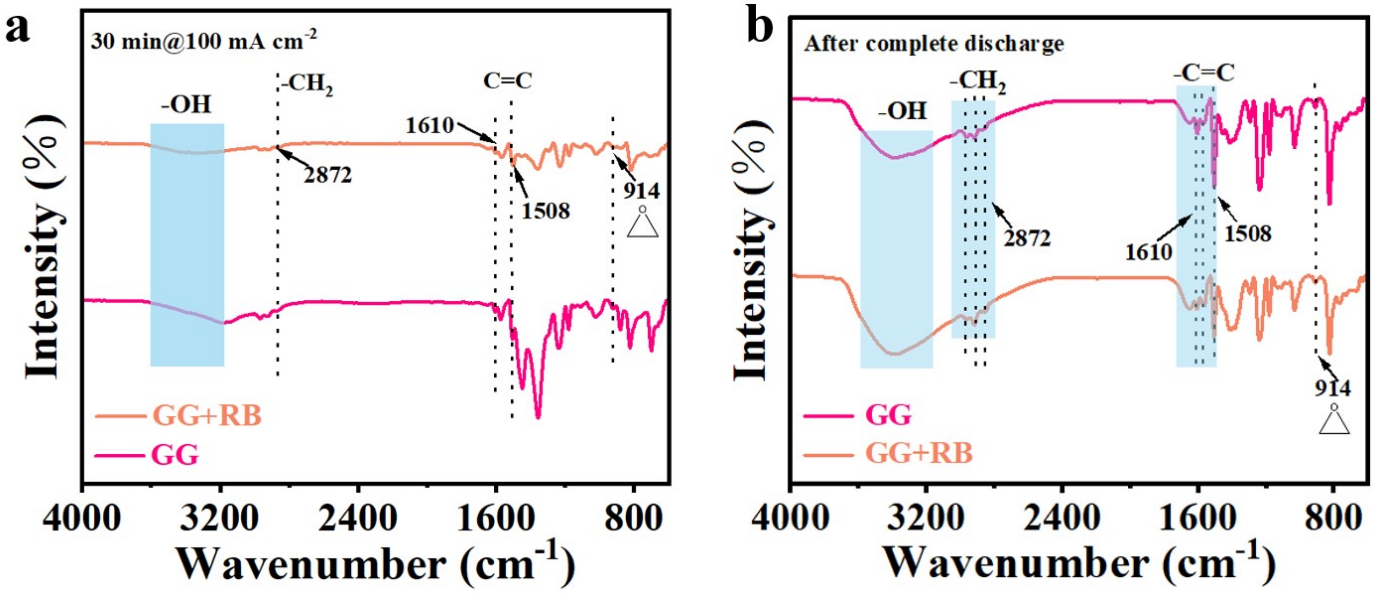

Figure S6. FTIR of GG and GG+RB discharge at (a) 100 mA cm^{-2} for 30 min and (b) completely.

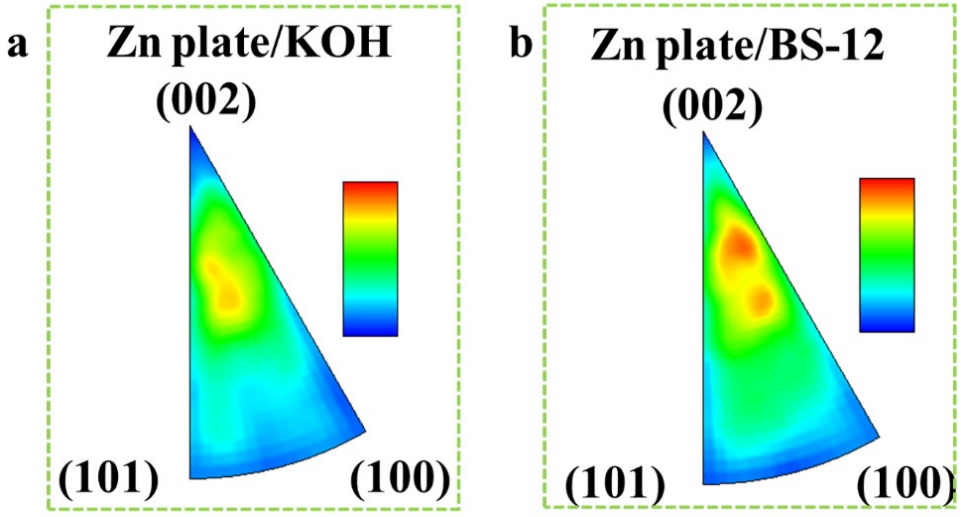

Figure S7. The EBSD inverse pole figures of (a) Zn plate/KOH and (b) Zn plate/RB.

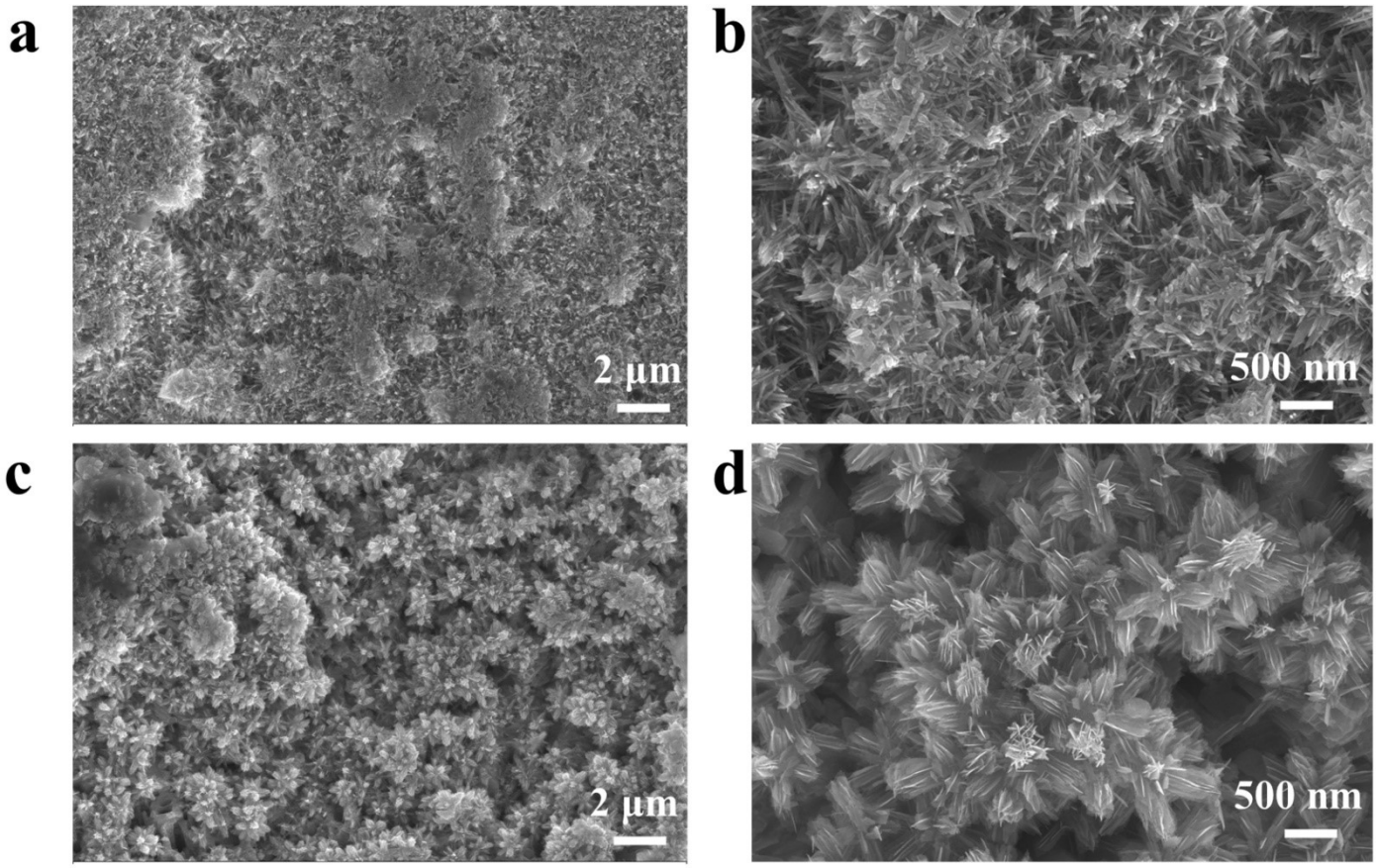

Figure S8. The SEM images of (a, b) Zn plate/KOH and (c, d) Zn plate/RB.

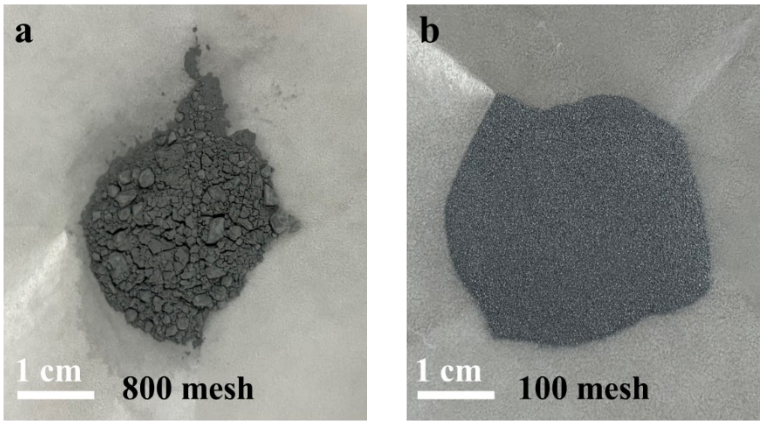

Figure S9. Optical photos of (a) 800 mesh and (b) 100 mesh Zn powder.

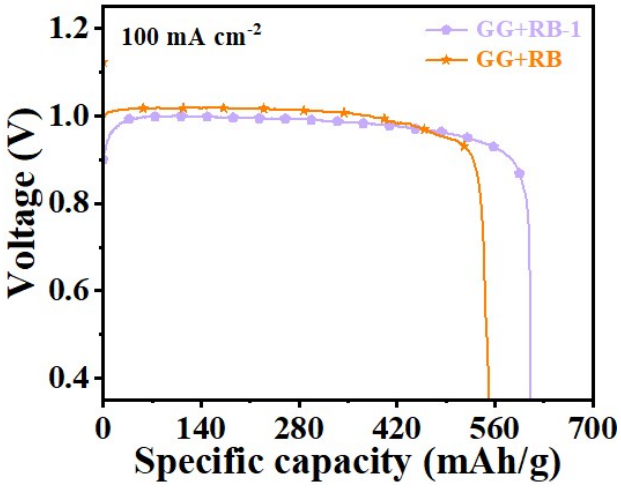

Figure S10. Galvanostatic discharge tests at 100 mA cm^{-2} using Zn powder of different mesh sizes.

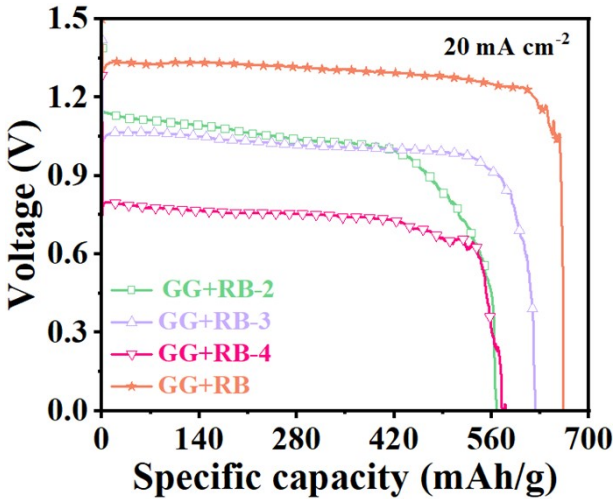

Figure S11. Galvanostatic discharge tests at 20 mA cm^{-2} using the E-44 binder with different contents.

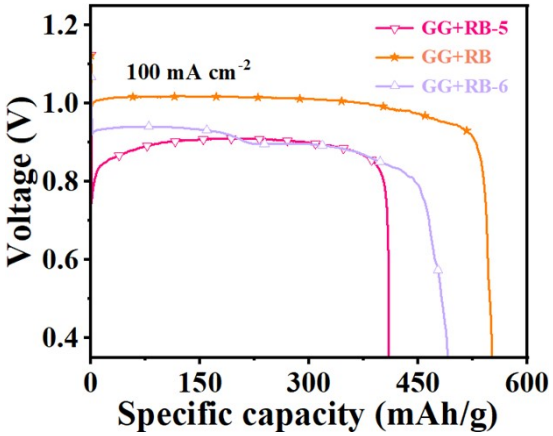

Figure S12. Galvanostatic discharge tests at 100 mA cm^{-2} using carbon black of different contents.

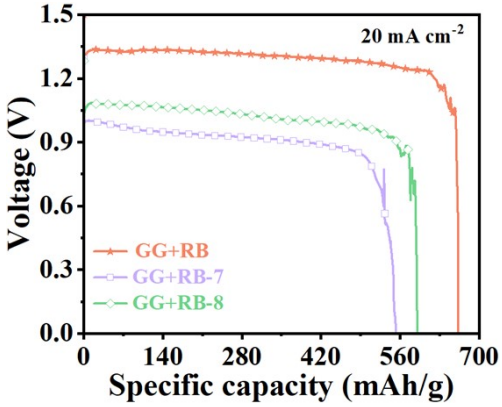

Figure S13. Galvanostatic discharge tests at 20 mA cm^{-2} using different types of conductive agents.

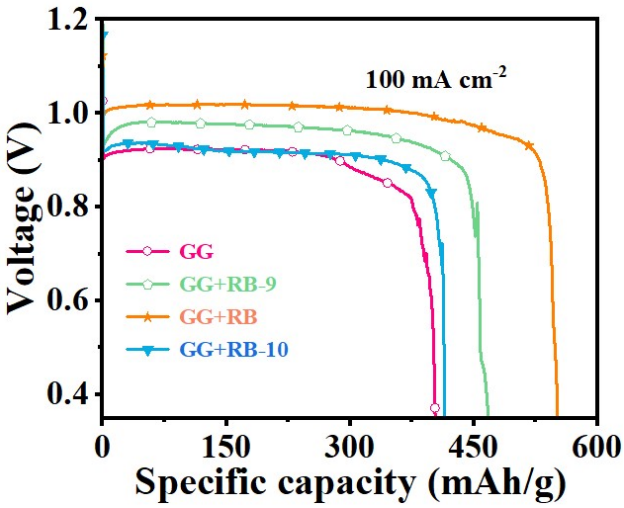

Figure S14. Galvanostatic discharge tests at 100 mA cm^{-2} using BS-12 of different contents.

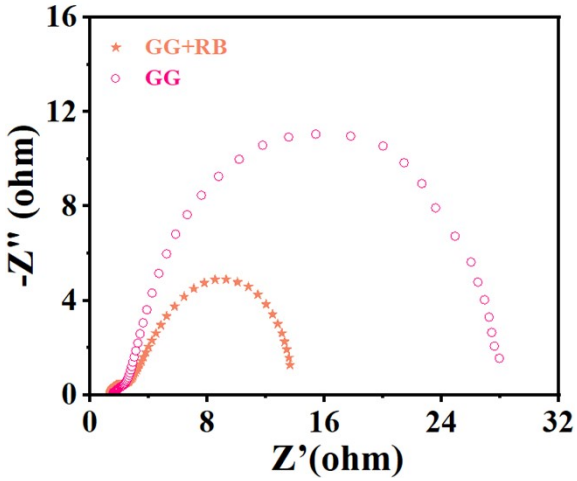

Figure S15. Nyquist plots of GG+RB and GG-based ZABs.

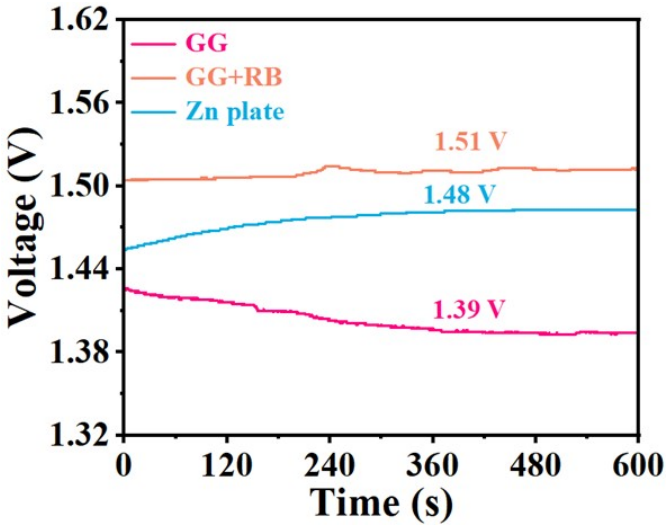

Figure S16. OCP of Zn plate, GG+RB, and GG-based ZABs.

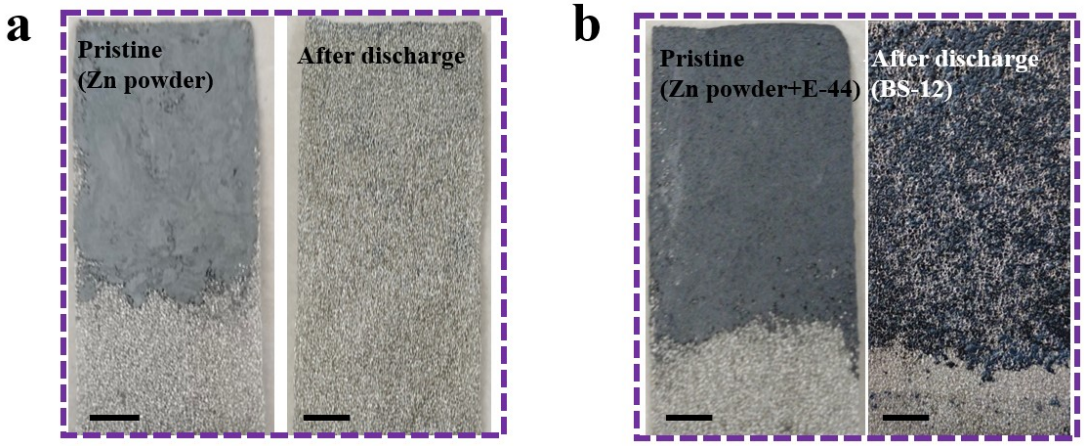

Figure S17. (a) The NB and (b) the GG+RB anode optical photos before and after discharge (Scale bar: 1 cm).

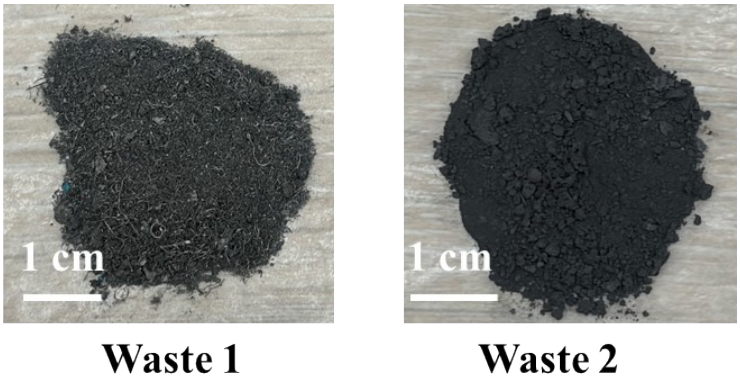

Figure S18. Optical photos of two different types of metal waste materials.

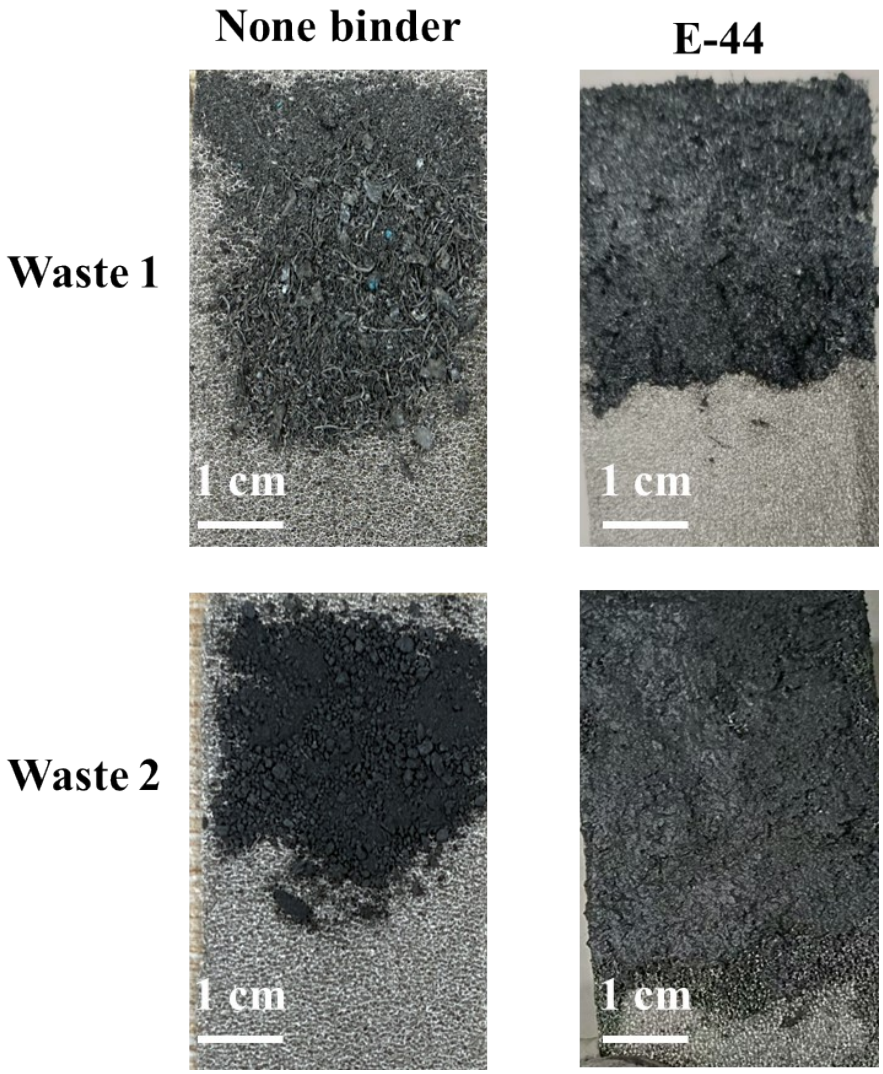

Figure S19. Optical photos of two different types of metal waste materials.

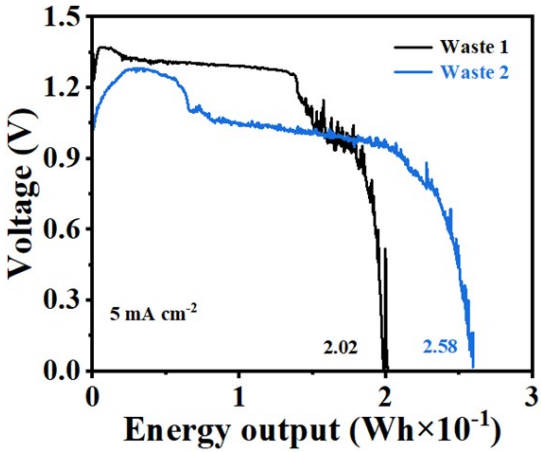

Figure S20. The electrical energy output of two types of metal dust waste materials.

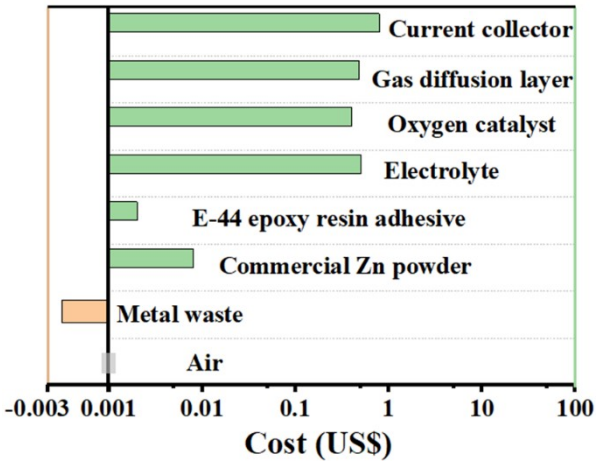

Figure S21. The cost of waste 2-air battery components.

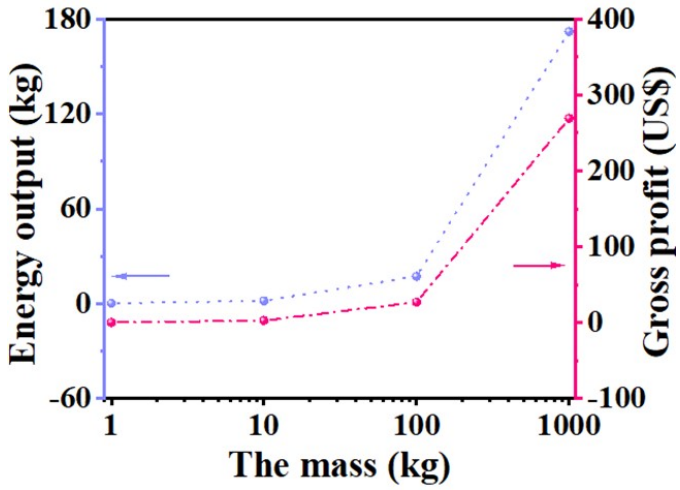

Figure S22. Correlation between estimated energy output, profit, and the mass of waste 2 in this work.

Table S1. Specific formulas for 19 samples (all of the following samples were obtained after discharge).

Samples	m(E-44)/g	m(C)/mg	Kinds of C	V(BS-12)/μL	Mesh
GG	0.5	50	Carbon black	0	800
GG+RB				10	
GG+RB-9				5	
GG+RB-10				25	
GG+RB-1	0.5	50	Carbon black	10	100
GG+RB-2	0.2	50	Carbon black	10	800
GG+RB-3	1				
GG+RB-4	1.5				
GG+RB-5	0.5	0	Carbon black	10	800
GG+RB-6		100			
GG+RB-7	0.5	50	CNT-3212	10	800
GG+RB-8	0.5		KS-6		
Zn plate/KOH	0.5	50	Carbon black	0	Zn plate
Zn plate/RB				10	
PTFE/RB	PTFE	50	Carbon black	10	800
PVDF/RB	PVDF				
CMC/RB	CMC				
PEG/RB	PEG				
NB	None	50	Carbon black	None	800
Waste 1	0.1	10	Carbon black	10	/
Waste 2					

Table S2. Original test data of Zeta potential.

Sample	Zeta potential (Mv)	Electrophoretic mobility (μm.cm/V.s)	Electric conductivity (mS/cm)	Wave length (nm)
GG-1	-18.7386	-1.4023	0.1209	671
GG-2	-18.0113	-1.4023	0.1209	
GG-3	-18.2280	-1.4191	0.1209	
GG+RB-1	-22.4546	-1.7482	0.0461	
GG+RB-2	-23.8554	-1.8572	0.0461	
GG+RB-3	-23.1593	-1.8031	0.0461	

Table S3. The performance comparison of reported ZABs.

Zn species	Open-circuit voltage (V)	Current density (mA cm^{-2})	Discharge voltage (V)	Utilization rate of Zn (%)	Ref.
Zn powder	1.52	20	1.33	80.7	This Work
Zn foil	/	20	1.203	75.79	[1]
Zn foil	1.4	10	1.1	77.4	[2]
Zn foil	1.428	20	1.17	79	[3]
Zn foil	1.36	1	1.3	77	[4]
Zn foil	1.5	2	1.22	66	[5]

Table S4. Chemical composition (wt%) of the waste 1 sample by XRF.

Fe	Al	O	Si	C	Cu	Zn	N	S	Ca	P	Mn	Pb	K	Cr
39.18	37.88	12.47	3.88	2.94	0.98	0.71	0.69	0.47	0.27	0.24	0.12	0.08	0.05	0.05

Table S5. Chemical composition (wt%) of the waste 2 sample by XRF.

Al	Si	Cu	Fe	Zn	Ca	Mn	P	Zr	Cr	K	Ni	Pb	S	Cl
78.48	9.06	4.71	2.63	2.11	0.84	0.57	0.36	0.19	0.17	0.16	0.13	0.12	0.12	0.10

Refrence

(1) Y. F. Li, A. J. Huang, L. X. Zhou, B. H. Li, M. Y. Zheng, Z. W. Zhuang, C. Chen, F. Y. Kang, and R. T. Lv, *Nat. Commun.*, 2024, ***15***, 8365.

(2) K. Z. Wu, L. Zhang, Y. F. Yuan, L. X. Zhong, Z. X. Chen, X. Chi, H. Lu, Z. H. Chen, R. Zou, T. Z. Li, C. Y. Jiang, Y. K. Chen, X. W. Peng, and J. Lu, *Adv. Mater.*, 2020, ***32***, 2002292.

(3) O. S. Jeon, E. S. Ko, Y. Y. Park, D. Hong, S. H. Lee, Y. P. Jeon, Y. La, S. Kim, I. S. Lee, G. S. Park, E. J. Lee, S. Kang, Y. J. Yoo, and S. Y. Park, *Adv. Energy Mater.*, 2023, ***13***, 2300285.

(4) Y. He, Y. F. Cui, J. W. Yu, W. X. Shang, and P. Tan, *Adv. Energy Mater.*, 2025, ***15***, 2405066.

(5) J. Y. Lyu, Q. Y. Zhou, H. F. Wang, Q. Xiao, Z. Qiang, X. P. Li, J. Wen, C. H. Ye, and M. F. Zhu, *Adv. Sci.*, 2023, ***10***, 2206591.